



**Providing Choice & Value**

Generic CT and MRI Contrast Agents



CONTACT REP

**AJNR**

This information is current as  
of July 17, 2025.

## **Increased Intracranial Arterial Pulsatility and Microvascular Brain Damage in Pseudoxanthoma Elasticum**









J.W. Bartstra, T. van den Beukel, G. Kranenburg, L.J.  
Geurts, A.M. den Harder, T. Witkamp, J.M. Wolterink,  
J.J.M. Zwanenburg, E. van Valen, H.L. Koek, W.P.T.M.  
Mali, P.A. de Jong, J. Hendrikse and W. Spiering

*AJNR Am J Neuroradiol* 2024, 45 (4) 386-392

doi: <https://doi.org/10.3174/ajnr.A8212>

<http://www.ajnr.org/content/45/4/386>

# Increased Intracranial Arterial Pulsatility and Microvascular Brain Damage in Pseudoxanthoma Elasticum

J.W. Bartstra,  T. van den Beukel, G. Kranenburg,  L.J. Geurts, A.M. den Harder, T. Witkamp,  J.M. Wolterink,  J.J.M. Zwanenburg,  E. van Valen, H.L. Koek, W.P.T.M. Mali,  P.A. de Jong,  J. Hendrikse, and  W. Spiering



## ABSTRACT

**BACKGROUND AND PURPOSE:** Carotid siphon calcification might contribute to the high prevalence of cerebrovascular disease in pseudoxanthoma elasticum through increased arterial flow pulsatility. This study aimed to compare intracranial artery flow pulsatility, brain volumes, and small-vessel disease markers between patients with pseudoxanthoma elasticum and controls and the association between arterial calcification and pulsatility in pseudoxanthoma elasticum.

**MATERIALS AND METHODS:** Fifty patients with pseudoxanthoma elasticum and 40 age- and sex-matched controls underwent 3T MR imaging, including 2D phase-contrast acquisitions for flow pulsatility in the assessment of ICA and MCA and FLAIR acquisitions for brain volumes, white matter lesions, and infarctions. All patients with pseudoxanthoma elasticum underwent CT scanning to measure siphon calcification. Flow pulsatility (2D phase-contrast), brain volumes, white matter lesions, and infarctions (3D T1 and 3D T2 FLAIR) were compared between patients and controls. The association between siphon calcification and pulsatility in pseudoxanthoma elasticum was tested with linear regression models.

**RESULTS:** Patients with pseudoxanthoma elasticum (mean age, 57 [SD, 12] years; 24 men) had significantly higher pulsatility indexes (1.05; range, 0.94–1.21 versus 0.94; range, 0.82–1.04;  $P = .02$ ), lower mean GM volumes (597 [SD, 53] mL versus 632 [SD, 53] mL;  $P < .01$ ), more white matter lesions (2.6; range, 0.5–7.5 versus 1.1; range, 0.5–2.4) mL;  $P = .05$ ), and more lacunar infarctions (64 versus 8,  $P = .04$ ) than controls (mean age, 58 [SD, 11] years; 20 men). Carotid siphon calcification was associated with higher pulsatility indexes in patients with pseudoxanthoma elasticum ( $\beta = 0.10$ ; 95% CI, 0.01–0.18).

**CONCLUSIONS:** Patients with pseudoxanthoma elasticum have increased intracranial artery flow pulsatility and measures of small-vessel disease. Carotid siphon calcification might underlie the high prevalence of cerebrovascular disease in pseudoxanthoma elasticum.

**ABBREVIATIONS:** CSVD = cerebral small-vessel disease; IEL = internal elastic lamina; LDL = low-density lipoprotein; PI = pulsatility index; PPI = inorganic pyrophosphate; PXE = pseudoxanthoma elasticum; RR = rate ratio; WML = white matter lesions


Pseudoxanthoma elasticum (PXE, Online Mendelian Inheritance in Man [OMIM] 264800) is a rare monogenetic disorder caused by mutations in the *ABCC6* gene, which result in degradation and calcification of the elastic fibers of the skin, the Bruch membrane in the eyes, and the peripheral arteries.<sup>1,2</sup> In the skin, this disorder results in yellow papules known as pseudoxanthomas. Calcification of the Bruch membrane results in peau d'orange, angioid streaks,

choroidal neovascularizations, and macular atrophy.<sup>3</sup> Arterial calcification of the peripheral arteries of the legs results in peripheral artery disease.<sup>4</sup> Patients with PXE are at increased risk of TIAs and strokes, and several case reports have confirmed increased white matter lesions (WML).<sup>5–7</sup> Recently, mutations in the *ABCC6* gene were implicated as one of the monogenetic causes of cerebral small-vessel disease (CSVD).<sup>8</sup> However, the underlying mechanisms that cause brain damage in PXE remain uncertain. Carotid hypoplasia,<sup>9</sup> vascular inflammation,<sup>10</sup> increased elastin degradation,<sup>11</sup> and calcification might all play a role. In addition to calcification of the legs, the intracranial carotid siphon is more frequently and severely calcified compared with the general population in PXE.<sup>2</sup> This intracranial calcification might underlie the increased prevalence of cerebrovascular disease in PXE. Recently, it was shown that the carotid siphon attenuates arterial pulsatility in the carotid artery in healthy volunteers<sup>12</sup> and patients with PXE.<sup>13</sup> Furthermore, it was found that calcification of the carotid siphon is related to increased

Received February 1, 2023; accepted after revision December 2.

From the Departments of Radiology (J.W.B., T.v.d.B., L.J.G., A.M.d.H., T.W., J.J.M.Z., W.P.T.M.M., P.A.d.J., J.H.), Vascular Medicine (G.K., W.S.), and Geriatrics (E.v.V., H.L.K.), University Medical Center Utrecht, Utrecht University, the Netherlands; and Department of Applied Mathematics (J.M.W., E.v.V., H.L.K.), Technical Medical Centre, University of Twente, Enschede, the Netherlands.

Please address correspondence to J.W. Bartstra, MD, Department of Radiology, University Medical Center Utrecht, Postbox 85500, 3508 GA Utrecht, the Netherlands; e-mail: jbartstra@hotmail.com

 Indicates article with online supplemental data.

<http://dx.doi.org/10.3174/ajnr.A8212>

pulsatility in the perforating arteries in patients with CSVD.<sup>14</sup> The burden of structural brain disease in PXE and the relation with structural and functional abnormalities in the brain vessels are unknown.

Arterial calcifications develop in the intimal and medial layers of the arterial wall. In the intima, they occur in atherosclerotic plaques and are a measure of the atherosclerotic involvement of the arterial bed.<sup>15</sup> In the medial layer, calcification of the internal elastic lamina (IEL) is shown to contribute to arterial stiffness.<sup>16,17</sup> Increased arterial stiffness reduces the physiologic Windkessel function of the arterial tree and allows increased pulsatility in end-organs like the brain.<sup>18</sup> Moreover in atherosclerotic plaques, arterial calcifications typically develop along the IEL and in the medial arterial wall in PXE.<sup>19</sup> We hypothesized that these carotid siphon calcifications might contribute to the high prevalence of cerebrovascular disease in PXE through increased arterial pulsatility. The aim of this study was to compare intracranial arterial flow pulsatility, brain volumes, infarctions, and WML between patients with PXE and controls. In addition, we investigated the association between carotid siphon calcification and arterial pulsatility, brain volumes, infarctions, and WML in patients with PXE.

## MATERIALS AND METHODS

### Study Design and Population

Patients were recruited from the Dutch National Expertise Center for PXE in the University Medical Center Utrecht. We conducted a patient-control study in 50 patients with PXE from the Dutch National Expertise Center for Pseudoxanthoma Elasticum (DNECP) who volunteered to participate and 40 healthy controls. All patients with PXE had a confirmed diagnosis of PXE. PXE was diagnosed if 2 of the following criteria were present: skin involvement (eg, yellow papules or plaques), eye involvement (eg, peau d'orange, angioid streaks), and genetic confirmation (biallelic *ABCC6* mutations).<sup>1</sup> Age- and sex-matched controls were recruited from the surrounding areas of patients with PXE. All patients with PXE and controls underwent MR imaging to assess brain structure and blood flow. Patients with PXE also underwent CT of the brain. Patients or controls were excluded if they were younger than 18 years of age, had an estimated glomerular filtration rate of  $<30 \text{ mL/min/1.73 m}^2$ , had a pacemaker or implantable cardioverter-defibrillator, had a metallic foreign body in the eye, or had claustrophobia. Controls were also excluded if they were first- or second-degree relatives of patients with PXE. The study was approved by the institutional review board of the University Medical Center Utrecht (No. 16–622/M-X), and written informed consent was obtained from all participants.

### Demographics

From all 50 patients and 40 controls, a medical history on medication and smoking status and a physical examination including height, weight, and blood pressure were obtained. Laboratory measurements included calcium, phosphate, estimated glomerular filtration rate, low-density lipoprotein (LDL) cholesterol, and 25-hydroxy vitamin D levels. Hypertension was defined as office systolic blood pressure of  $>140 \text{ mm Hg}$  and/or office diastolic blood pressure of  $>90 \text{ mm Hg}$  and/or the use of antihypertensive drugs. Hypercholesterolemia was defined as statin use and/or an LDL cholesterol level of  $>2.5 \text{ mmol/L}$ .

### CT Acquisition and Processing

Calcification was visualized on unenhanced, thin-section CT scans (120 kV[peak], mAs depending on body weight) on a Biograph 40 (Siemens) or a Brilliance CT 64 (Philips Healthcare) scanner. The carotid siphon calcification relative mass score was quantified using an in-house-developed software tool (iX Viewer; Image Sciences Institute) on the basis of the area and density of arterial wall lesions with an attenuation of  $>130 \text{ HU}$  (J.W.B.).<sup>20</sup> Twenty-five randomly selected scans were scored by 2 investigators. The intraclass correlation coefficient was assessed and was excellent (0.915; range, 0.751–0.966).

### MR Imaging Acquisition and Processing

Fifty patients with PXE and 42 healthy controls underwent a standardized MR imaging protocol (Ingenia CX 3T; Philips Healthcare) including time-resolved 2D phase-contrast, 3D T1-weighted, and 3D T2-weighted FLAIR acquisitions of the brain. In 2 controls, MR imaging was ended prematurely due to claustrophobia.

The 2D phase-contrast acquisitions were planned separately for both sides proximal and distal to the carotid siphon at the cavernous ICA segment (C4) and at the origin of the MCA M1 segment, respectively (Online Supplemental Data).<sup>21,22</sup> We used the following imaging parameters: FOV =  $250 \times 250 \text{ mm}^2$ , acquired resolution =  $0.5 \times 0.5 \times 3 \text{ mm}^3$  (reconstructed spatial resolution =  $0.25 \times 0.25 \times 3 \text{ mm}^3$ ), acquired temporal resolution = 64 ms, and unidirectional through-plane velocity-encoding sensitivities = 100 cm/s for C4 and MCA. The flow acquisitions provided time-resolved measurements of the blood flow velocity and volumetric flow rates over the cardiac cycle.

An in-house-developed Matlab script (MathWorks) was used to process the 2D phase-contrast acquisitions. The script created ROIs for each phase of the cardiac cycle based on image intensity and corrected potential phase wraps in the velocity maps. All ROIs were manually checked for ROI variation (L.J.G.). The acquisitions were included if they met the following previously described quality criteria.<sup>12</sup> The image section was planned perpendicular to the vessel (circular vessel appearance), the contour of the ROI followed the vessel contour adequately (circular ROI), and the contour was stable over the cardiac cycle with only minor ROI variations. From the included acquisitions, blood flow was calculated by integrating blood flow velocity over the vessel lumen. Next, the pulsatility index (PI) was calculated as peak systolic flow minus the lowest diastolic flow divided by the mean flow during 1 cardiac cycle.<sup>21</sup> The mean PI was calculated from the left and right carotid siphon and MCA. Of 360 pulsatility measurements, 35 were missing due to scan artifacts or suboptimal planning, and data were imputed using a single imputation. These measurements were previously shown to be reproducible among observers.<sup>21</sup>

Brain volumes (GM, WM, CSF, and cortical thickness) and WML were computed automatically from the 3D T1 and 3D T2 FLAIR sequences using the Computational Anatomy Toolbox 12 (CAT12, <http://www.neuro.uni-jena.de/cat/>) and the Lesion Segmentation Tool (LST, <https://www.applied-statistics.de/lst.html>) within SPM12 software (<https://www.fil.ion.ucl.ac.uk/spm/software/spm12/>). WML were quantified on the T2 FLAIR scans using LST, and the T1 scans were used to quantify the other brain volumes using CAT12. Before segmentation with CAT12, the WML on T1 scans

**Table 1: Clinical characteristics of 50 patients with PXE and 40 controls<sup>a</sup>**

Characteristics	PXE (n = 50)	Controls (n = 40)	P Value
Clinical			
Age (yr)	57 (SD, 12)	58 (SD, 11)	.49
Male sex (No.)	24 (48)	20 (50)	.85
BMI (kg/m <sup>2</sup> )	26 (SD, 4)	26 (SD, 4)	.74
Current smokers (No.)	6 (12)	5 (13)	.86
Systolic blood pressure (mm Hg)	136 (SD, 21)	133 (SD, 15)	.49
Diastolic blood pressure (mm Hg)	77 (SD, 12)	79 (SD, 10)	.41
Hypertension (No.)	22 (44)	18 (45)	.92
Hypercholesterolemia (No.)	43 (86)	37 (93)	.33
Medication			
Glucose-lowering medication (No.)	1 (2)	0 (0)	.38
Antihypertensive medication (No.)	13 (26)	7 (18)	.40
Cholesterol-lowering medication (No.)	26 (52)	5 (13)	<.01
Laboratory			
Calcium (mmol/L)	2.38 (SD, 0.09)	2.39 (SD, 0.09)	.61
Phosphate (mmol/L)	1.02 (SD, 0.16)	0.98 (SD, 0.16)	.25
Estimated glomerular filtration rate (mL/min/1.73m <sup>2</sup> )	90 (82–90)	88 (75–90)	.17
LDL-cholesterol (mmol/L)	2.8 (SD, 0.9)	3.6 (SD, 0.8)	<.01
25-OH vitamin D (nmol/L)	74 (SD, 36)	61 (SD, 20)	.04

**Note:**—BMI indicates body mass index; 25-OH vitamin D = 25-hydroxy vitamin D.

<sup>a</sup>Data are presented as mean (SD), median (interquartile range), or No. (%) when appropriate. Data were analyzed using the Student *t* test, Mann Whitney *U* test, or  $\chi^2$  test when appropriate. A *P* value < .05 was statistically significant.



**FIG 1.** Clinical example of vascular and brain disease in PXE. Carotid siphon calcification on CT (A, red circles) and small-vessel disease on 3T MR imaging (B). The blue arrow shows a lacunar infarction; the orange arrows show WML.

were filled on the basis of the results of the LST segmentation. All segmentations were visually checked (J.W.B.). Lacunar, subcortical, and cortical infarctions were scored on the basis of the Standards for Reporting Vascular changes on nEuroimaging recommendations<sup>23</sup> on the 3D T1 and 3D T2-FLAIR scans by an experienced, independent neuroradiologist blinded to the disease state, demographics, calcification mass, and pulsatility index (T.W.).

### Statistical Analysis

Descriptive data are presented as categorical (number and percentage), normally distributed continuous (mean [SD]), or non-normally distributed continuous variables (median [interquartile range]) as appropriate.

The difference in the PI, brain volumes, and small-vessel disease burden between patients with PXE and healthy controls was evaluated with the unpaired Student *t* test with 2-tailed probabilities when normally distributed or the Mann-Whitney *U* test when non-normally distributed. Separate analyses were performed for lacunar infarctions and all infarctions, in which lacunar, subcortical, and cortical infarctions were summed.

<sup>10</sup>Log transformation was performed on the carotid siphon calcification mass. Linear regression models were built to test the association between calcification mass and the PI and brain volumes and small-vessel disease. Negative binomial regression models were built to test the association between carotid siphon calcification and lacunar and all infarctions. The different models were adjusted for age and sex and for age, sex, and hypertension. A *P* value < .05 was statistically significant. Data analyses were performed in SPSS statistics, Version 25 (IBM); figures were made in R statistical and computing software, Version 3.3.2 (<http://www.r-project.org/>).

## RESULTS

### Baseline Characteristics

The baseline characteristics of the 50 patients with PXE and 40 healthy controls are presented in Table 1. The mean age of patients with PXE was 57 versus 58 years in controls. Forty-eight percent of patients with PXE versus 50% of controls were men. The PI measurement of 1 patient with PXE was excluded because of an ophthalmic artery aneurysm, which might affect blood flow. The brain volume measurements from 2 patients with PXE were

excluded from analysis due to demyelinating disease and a communicating hydrocephalus.

### Imaging Findings in Those with PXE versus Controls

We provide an illustration of the disease on CT and MR imaging in 1 of the patients with PXE in Fig 1. The median PI was significantly higher in patients with PXE than in controls (1.05; range, 0.94–1.21 versus 0.94; range, 0.82–1.04; *P* = .01) (Table 2). Patients with PXE had significantly lower mean GM volumes (597 [SD, 53] mL versus 632 [SD, 53] mL, *P* < .01) and more WML (2.6; range, 0.5–7.5 mL versus 1.1; range, 0.5–2.4; *P* = .05). Patients with PXE had more lacunar infarctions (total 64 versus 8, *P* = .04) and all types of infarctions (75 versus 14, *P* = .02).



## Arterial Calcification, Flow Pulsatility, and Small-Vessel Disease in PXE

Forty-eight of 50 (96%) patients with PXE had calcifications in the carotid siphon, and the median calcification mass score was 17 (range, 7–51). Calcification was associated with a higher PI ( $\beta = 0.10$ ; 95% CI, 0.01–0.18; Fig 2), higher CSF volume ( $\beta = 67.1$ ; 95% CI, 18.7–115.5), more WML ( $\beta = 6.2$ ; 95% CI, 1.6–10.9), and all infarctions (rate ratio [RR] = 2.8; 95% CI, 1.1–7.0) when adjusted for age, sex, and hypertension (Table 3). The PI was associated with more WML (Table 4).

## DISCUSSION

In this patient-control study, we show that patients with PXE have higher intracranial artery flow pulsatility, lower GM volumes, and

more lacunar infarctions and WML as a measure of CSVD, compared with an age- and sex-matched control population. In addition, we show that carotid siphon calcification in patients with PXE is associated with higher flow pulsatility of the intracranial arteries and that calcification is associated with reduced brain volumes and a higher small-vessel disease burden. These findings support the pulsatility hypothesis and show that arterial calcification is associated with brain damage in PXE (Fig 3). This pulsatility hypothesis states that increased pulsatility of the blood flow to the brain can damage brain tissue.<sup>18</sup> Large elastic arteries such as the aorta and carotid artery expand during systole and thereby dampen the pulsatile blood flow to the brain. This dampening results in laminar blood flow in the small vessels of the brain. Stiffening of the large arteries results in less dampening of the pulsatile blood flow and, therefore, increased pulsatility in the microvasculature, which might damage the brain parenchyma.

Arterial calcification is thought to contribute to arterial stiffening. These calcifications develop in the intimal and medial layers of the arterial wall.<sup>16</sup> Intimal calcifications occur in atherosclerotic plaques and are suggested to contribute to plaque stabilization. IEL calcification is mainly thought to contribute to arterial stiffness and hypertension and might cause increased pulsatility in high-flow organs such as the kidney and the brain.<sup>18</sup> Carotid siphon calcification is very prevalent in the general population in which it co-occurs, with atherosclerotic intimal calcification.<sup>24</sup> It is, therefore, difficult to investigate the effect of IEL calcifications in cardiovascular disease in general populations. Arterial calcifications in PXE typically develop along the IEL in the medial arterial wall.<sup>19</sup> Although patients with PXE do develop atherosclerotic calcifications, these are not considered to be more than in the general population. PXE can, therefore, be seen as a model disease for the role of relatively isolated IEL calcifications in cardiovascular disease.

The findings of this study are in line with those in previous research in more specific and general populations. A study on patients with ischemic stroke showed that intracranial artery calcification is correlated with increased arterial pulsatility in the MCA as measured with ultrasound.<sup>25,26</sup> Intracranial artery calcifications are associated with small-vessel disease,<sup>27</sup> infarctions,<sup>28</sup> decreased brain volumes,<sup>27</sup> dementia, and cognitive decline in the general and aging

**Table 2: Imaging findings in patients with PXE compared with controls<sup>a</sup>**

	Patients with PXE (n = 50)	Controls (n = 40)	P Value
Carotid siphon			
Calcification mass score	17 (7–51)	—	—
PI	1.05 (0.94–1.21)	0.94 (0.82–1.04)	.02 <sup>b</sup>
Brain MR imaging markers			
GM (mL)	597 (SD, 53)	632 (SD, 53)	<.01 <sup>c</sup>
WM (mL)	492 (SD, 52)	509 (SD, 56)	.15
CSF (mL)	337 (SD, 104)	311 (SD, 82)	.18
Cortical thickness (mm)	2.6 (SD, 0.1)	2.6 (SD, 0.1)	.16
WML (mL)	2.6 (0.5–7.5)	1.1 (0.5–2.4)	.05 <sup>b</sup>
Infarctions			
Lacunar infarctions			
No. of patients	16 (32)	6 (15)	.06
No. of infarctions	64	8	.04 <sup>b</sup>
All infarctions			
No. of patients	19 (38)	7 (18)	.03 <sup>b</sup>
No. of infarctions	75	14	.02 <sup>b</sup>

**Note:**—The en dash indicates that data on calcification mass are not available for controls.

<sup>a</sup> Data are presented as mean (SD), median (interquartile range), or No. (%) when appropriate. Data were analyzed using the Student *t* test, Mann-Whitney *U* test, or  $\chi^2$  test when appropriate. All infarctions include lacunar infarctions, 3 subcortical and 8 cortical infarctions in patients with PXE, and 6 cortical infarctions in controls.  $P < .05$  was statistically significant.

<sup>b</sup>  $P < .05$ .

<sup>c</sup>  $P < .01$ .

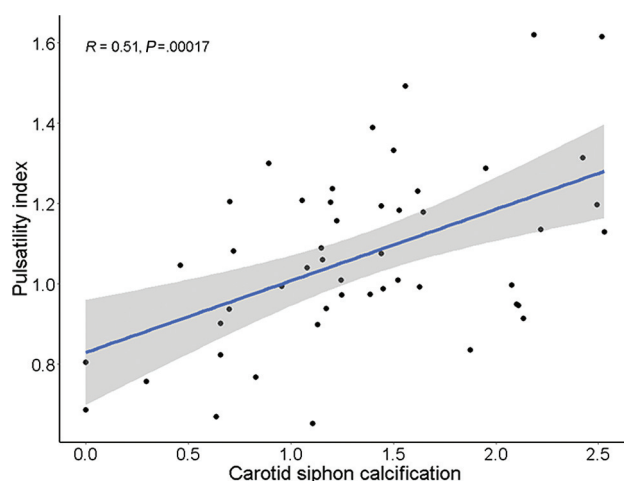


**FIG 2.** Correlation between carotid siphon calcification and the PI in patients with PXE. Carotid siphon calcification was correlated with the intracranial PI ( $R = 0.51$ ,  $P < .01$ , regression line; 95% CI, gray band). This association remained significant after multivariate adjustment for age and sex ( $\beta = 0.10$ ; 95% CI, 0.02–0.18\*) and age, sex, and hypertension ( $\beta = 0.10$ ; 95% CI, 0.01–0.18\*). Carotid siphon calcification was analyzed as  $10 \log (1 + \text{carotid siphon calcification})$ .  $P < .05$  was statistically significant. A single asterisk indicates  $P < .05$ .

**Table 3: Associations of carotid siphon calcification with brain MR imaging findings<sup>a</sup>**

	Carotid Siphon Calcification in PXE	
	Age- and Sex-Adjusted (n = 50)	Multivariable-Adjusted (n = 50)
MR imaging volumes ( $\beta$ [95% CI])		
GM (mL)	-17.3 [-39.9–5.2]	-16.8 [-39.9–6.4]
WM (mL)	-3.6 [-27.3–20.2]	-4.2 [-28.4–20.0]
CSF (mL)	74.7 [25.5–123.9] <sup>c</sup>	67.1 [18.7–115.5] <sup>c</sup>
Cortical thickness ( $\mu$ m)	-39.8 [-89.9–10.1]	-40.5 [-91.6–10.7]
WML (mL)	6.4 [1.9–11.0] <sup>c</sup>	6.2 [-1.6–10.9] <sup>b</sup>
Brain infarctions (RR [95% CI])		
Lacunar infarctions	2.5 [0.98–6.4]	2.3 [0.9–6.1]
All infarctions	3.1 [1.3–7.5] <sup>b</sup>	2.8 [-1.1–7.0] <sup>b</sup>

<sup>a</sup> Carotid siphon calcifications are analyzed as  $^{10}\log 1 + \text{carotid siphon calcification}$ . For carotid siphon calcification, MR imaging volumes and infarctions are adjusted for age and sex (model 1) and age, sex, and hypertension (model 2).  $P < .05$  was statistically significant.

<sup>b</sup>  $P < .05$ .

<sup>c</sup>  $P < .01$ .

**Table 4: Associations of pulsatility with brain MR imaging findings<sup>a</sup>**

	Pulsatility in PXE	
	Age and Sex-Adjusted (n = 50)	Multivariable-Adjusted (n = 50)
MR imaging volumes ( $\beta$ [95% CI])		
GM (mL)	3.8 [-73.9–81.6]	7.4 [-71.4–86.1]
WM (mL)	22.7 [-55.8–101.3]	23.1 [-57.0–103.2]
CSF (mL)	68.6 [-115.5–252.7]	45.6 [-131.8–223.0]
Cortical thickness ( $\mu$ m)	29.5 [-145.0–204.1]	31.9 [-146.0–209.7]
WML (mL)	26.5 [11.6–41.3] <sup>c</sup>	25.9 [10.8–40.9] <sup>c</sup>
Brain infarctions (RR [95%CI])		
Lacunar infarctions	1.7 [0.1–23.6]	1.8 [0.1–25.0]
All infarctions	2.3 [0.2–1.2]	2.5 [0.2–33.6]

<sup>a</sup> For pulsatility, MR imaging volumes and infarctions are adjusted for age and sex (model 1) and age, sex, and hypertension (model 2).  $P < .05$  was statistically significant.

<sup>b</sup>  $P < .05$ .

<sup>c</sup>  $P < .01$ .

populations.<sup>27,29</sup> Increased pulsatility is associated with brain atrophy in the elderly and in patients along the dementia spectrum<sup>30,31</sup> and with small-vessel disease in patients with an acute stroke or TIA.<sup>32</sup> These findings suggest that arterial calcification and increased pulsatility might also play a role in brain damage in more general populations. Recently, we developed a histologic validated CT calcium score to differentiate between a dominant pattern of atherosclerotic intimal calcification and IEL calcification in the CS for use in the general population.<sup>33</sup> This score was used in 2 studies from the general population of the Rotterdam study. It showed that IEL calcification increases from 23% below 65 years of age to 79% above 80 years of age.<sup>34</sup> Furthermore, it was shown that in the general population, IEL calcification of the carotid siphon (CS) is the leading mechanism explaining the link between blood pressure and CSVD.<sup>35</sup> Second, IEL calcification was more strongly associated with stroke than intimal calcification, certainly in the elderly population.<sup>34</sup> Longitudinal studies that modify calcification or pulsatility are needed to provide further causal evidence.<sup>36</sup> We performed a patient-control study in a calcific disease, PXE, and our findings support the hypothesis, but we cannot claim causality on the basis of this cross-sectional study.

In PXE, low levels of inorganic pyrophosphate (PPi) are thought to underlie the increased propensity for arterial calcification.<sup>37</sup> PPi is a potent calcification inhibitor that also plays an important role in other genetic disorders like generalized arterial calcification of infancy (OMIM 208000) and arterial calcification due to a deficiency in CD73 (OMIM #211800).<sup>16</sup> In generalized arterial calcification of infancy, the complete lack of PPi results in extensive arterial calcification at birth, which is often lethal in the first half year of life.<sup>16</sup> Arterial calcification due to a deficiency in CD73 results in extensive calcification of the arteries and the joints of the hands and feet.<sup>16</sup> The low levels of PPi in PXE result in ectopic calcification of the skin, eyes, and arteries.<sup>1</sup> Recent studies for the treatment of PXE focus on increasing PPi with oral supplementation,<sup>38</sup> preventing PPi degradation by inhibiting tissue-nonspecific alkaline phosphatase,<sup>39</sup> or supplying the stable PPi analog etidronate.<sup>40,41</sup> Although all are promising studies, long-term longitudinal data on the effect of these therapies on arterial calcification progression, pulsatility, or clinical outcomes are currently lacking.

### Strengths and Limitations

A strength of this study is the extensive imaging. We used CT and functional and structural MR imaging to test every step from our hypothesis from large-artery carotid siphon calcification to microvascular brain damage.

Because we did not obtain CT scans of the healthy controls, the difference in carotid siphon calcifications could not be assessed. However, it was previously shown that the prevalence and severity of carotid siphon calcification are higher in patients with PXE than in hospital controls.<sup>2</sup> In this cohort, patients with PXE were more often on statin treatment than the healthy controls. Because of their increased cardiovascular risk, patients with PXE in our clinical practice are started on statin treatment early to control additional cardiovascular risk factors. The healthy controls had significantly higher LDL cholesterol levels. To compare the prevalence of hypercholesterolemia between the groups, we, therefore, made a composite hypercholesterolemia score based on statin use and an LDL cholesterol level of  $>2.5$  mmol/L; the score showed no differences between the groups. In addition, patients with PXE had significantly lower vitamin D levels. Adjustment of the regression models for LDL cholesterol, statin treatment, and vitamin D levels did not significantly change the outcomes of the study. Finally, we performed a cross-sectional study that supports the pulsatility hypothesis; however, causal

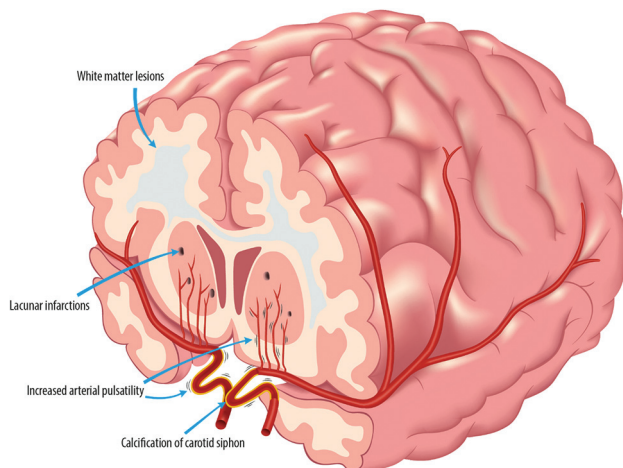


**FIG 3.** Arterial calcification, pulsatility, and microvascular brain damage in PXE. Carotid siphon calcification as a measure of intracranial arterial calcification is associated with increased flow pulsatility in PXE. The subsequent pulse pressure–induced microvascular damage, including lacunar infarctions and WML, might contribute to cognitive decline.

claims can only be proved in longitudinal studies, preferably with an intervention that modifies the pulsatility. Also, the calcification-induced change in arterial pulsatility occurs locally and is transmitted more by downward flow toward the cerebral tissue. Thus, in this later trajectory, the pulsatility can be modulated again. Thus, another way to more certainly assess whether pulsatility reaches the cerebral tissue is by measuring the pulsatility in perforating arteries.

In our controls, we observed lacunar infarctions in 6 (15%), which appears somewhat higher than those observed in the Rotterdam study (7.6%). This finding could be explained by the sensitivity of the method (ie, we used 3T instead of 1.5T) or by the small sample size of our control group.<sup>42</sup> Due to the cross-sectional design, caution is needed with causal assumptions. Larger and longitudinal studies in other populations must show whether our results are generalizable and whether progression of carotid siphon calcification results in progression of microvascular brain damage in patients with PXE and other populations.

## CONCLUSIONS

We showed that patients with PXE have more structural brain disease and increased intracranial arterial flow pulsatility compared with healthy controls. Arterial calcification of the carotid siphon is associated with increased flow pulsatility and microvascular brain damage, including infarctions and WML in patients with PXE. Larger, longitudinal studies are needed to further elucidate the causal role of arterial calcification and pulsatility in PXE-related brain disease.

Disclosure forms provided by the authors are available with the full text and PDF of this article at [www.ajnr.org](http://www.ajnr.org).

## REFERENCES

- Plomp AS, Toonstra J, Bergen AA, et al. **Proposal for updating the pseudoxanthoma elasticum classification system and a review of the clinical findings.** *Am J Med Genet A* 2010;152A:1049–58 [CrossRef](#) [Medline](#)
- Kranenburg G, de Jong PA, Mali WP, et al. **Prevalence and severity of arterial calcifications in pseudoxanthoma elasticum (PXE) compared to hospital controls: novel insights into the vascular phenotype of PXE.** *Atherosclerosis* 2017;256:7–14 [CrossRef](#) [Medline](#)
- Risseuw S, Ossewaarde-van Norel J, van Buchem C, et al. **The extent of angioid streaks correlates with macular degeneration in pseudoxanthoma elasticum.** *Am J Ophthalmol* 2020;220:82–90 [CrossRef](#) [Medline](#)
- Leftheriotis G, Kauffenstein G, Hamel JF, et al. **The contribution of arterial calcification to peripheral arterial disease in pseudoxanthoma elasticum.** *PLoS One* 2014;9:e96003 [CrossRef](#) [Medline](#)
- Kauw F, Kranenburg G, Kappelle LJ, et al. **Cerebral disease in a nationwide Dutch pseudoxanthoma elasticum cohort with a systematic review of the literature.** *J Neurol Sci* 2017;373:167–72 [CrossRef](#) [Medline](#)
- Cerrato P, Giraudo M, Baima C, et al. **Asymptomatic white matter ischemic lesions in a patient with pseudoxanthoma elasticum.** *J Neurol* 2005;252:848–49 [CrossRef](#) [Medline](#)
- Pavlovic AM, Zidverc-Trajkovic J, Milovic MM, et al. **Cerebral small vessel disease in pseudoxanthoma elasticum: three cases.** *Can J Neurol Sci* 2005;32:115–18 [CrossRef](#) [Medline](#)
- Manini A, Pantoni L, Pantoni L, et al. **Genetic causes of cerebral small vessel diseases: a practical guide for neurologists.** *Neurology* 2022;100:766–83 [CrossRef](#) [Medline](#)
- Omarjee L, Fortrat JO, Larralde A, et al. **Internal carotid artery hypoplasia: a new clinical feature in pseudoxanthoma elasticum.** *J Stroke* 2019;21:108–11 [CrossRef](#) [Medline](#)
- Mention PJ, Lacoëuille F, Leftheriotis G, et al. **18F-fluorodeoxyglucose and 18F-sodium fluoride positron emission tomography/computed tomography imaging of arterial and cutaneous alterations in pseudoxanthoma elasticum.** *Circ Cardiovasc Imaging* 2018;11:e007060 [CrossRef](#) [Medline](#)
- Bartstra JW, Spiering W, van den Ouweland JM, et al. **Increased elastin degradation in pseudoxanthoma elasticum is associated with peripheral arterial disease independent of calcification.** *J Clin Med* 2020;9:2771–11 [CrossRef](#) [Medline](#)
- van Tuijl RJ, Ruigrok YM, Velthuis BK, et al. **Velocity pulsatility and arterial distensibility along the internal carotid artery.** *J Am Heart Assoc* 2020;9:e016883 [CrossRef](#) [Medline](#)
- Bartstra JW, van Tuijl RJ, de Jong PA, et al. **Pulsatility attenuation along the carotid siphon in pseudoxanthoma elasticum.** *AJNR Am J Neuroradiol* 2021;42:2030–33 [CrossRef](#) [Medline](#)
- van Tuijl RJ, Ruigrok YM, Geurts LJ, et al. **Does the internal carotid artery attenuate blood-flow pulsatility in small vessel disease? A 7 T 4D-flow MRI study.** *J Magn Reson Imaging* 2022;56:527–35 [CrossRef](#) [Medline](#)
- Panh L, Lairez O, Ruidavets JB, et al. **Coronary artery calcification: from crystal to plaque rupture.** *Arch Cardiovasc Dis* 2017;110:550–61 [CrossRef](#) [Medline](#)
- Lanzer P, Boehm M, Sorribas V, et al. **Medial vascular calcification revisited: review and perspectives.** *Eur Heart J* 2014;35:1515–25 [CrossRef](#) [Medline](#)
- Chirinos JA, Segers P, Hughes T, et al. **Large-artery stiffness in health and disease: JACC State-of-the-Art Review.** *J Am Coll Cardiol* 2019;74:1237–63 [CrossRef](#) [Medline](#)
- Mitchell GF. **Aortic stiffness, pressure and flow pulsatility, and target organ damage.** *J Appl Physiol (1985)* 2018;125:1871–80 [CrossRef](#) [Medline](#)
- Vos A, Kranenburg G, de Jong PA, et al. **The amount of calcifications in pseudoxanthoma elasticum patients is underestimated in computed tomographic imaging; a post-mortem correlation of histological and computed tomographic findings in two cases.** *Insights Imaging* 2018;9:493–98 [CrossRef](#) [Medline](#)
- Hoffmann U, Kwait DC, Handwerker J, et al. **Vascular calcification in ex vivo carotid specimens: precision and accuracy of measurements**

- with multi-detector row CT. *Radiology* 2003;229:375–81 [CrossRef Medline](#)
21. Correia de Verdier M, Wikstrom J. Normal ranges and test-retest reproducibility of flow and velocity parameters in intracranial arteries measured with phase-contrast magnetic resonance imaging. *Neuroradiology* 2016;58:521–31 [CrossRef Medline](#)
  22. Buijs PC, Krabbe-Hartkamp MJ, Bakker CJ, et al. Effect of age on cerebral blood flow: measurement with ungated two-dimensional phase-contrast MR angiography in 250 adults. *Radiology* 1998;209:667–74 [CrossRef Medline](#)
  23. Wardlaw JM, Smith EE, Biessels GJ, et al; STRIVE v1. Neuroimaging standards for research into small vessel disease and its contribution to ageing and neurodegeneration. *Lancet Neurol* 2013;12:822–38 [CrossRef Medline](#)
  24. Bartstra JW, van den Beukel TC, Van Hecke W, et al. Intracranial arterial calcification: prevalence, risk factors, and consequences: JACC Review Topic of the Week. *J Am Coll Cardiol* 2020;76:1595–604 [CrossRef Medline](#)
  25. Wu X, Wang L, Zhong J, et al. Impact of intracranial artery calcification on cerebral hemodynamic changes. *Neuroradiology* 2018;60:357–63 [CrossRef Medline](#)
  26. Park KY, Chung PW, Kim YB, et al. Increased pulsatility index is associated with intracranial arterial calcification. *Eur Neurol* 2013;69:83–88 [CrossRef Medline](#)
  27. Bos D, Vernooij MW, Elias-Smale SE, et al. Atherosclerotic calcification relates to cognitive function and to brain changes on magnetic resonance imaging. *Alzheimers Dement* 2012;8:S104–111 [CrossRef Medline](#)
  28. Hong NR, Seo HS, Lee YH, et al. The correlation between carotid siphon calcification and lacunar infarction. *Neuroradiology* 2011;53:643–49 [CrossRef Medline](#)
  29. Bos D, Vernooij MW, de Bruijn RF, et al. Atherosclerotic calcification is related to a higher risk of dementia and cognitive decline. *Alzheimers Dement* 2015;11:639–47.e1 [CrossRef Medline](#)
  30. Berman SE, Rivera-Rivera LA, Clark LR, et al. Intracranial arterial 4D-flow is associated with metrics of brain health and Alzheimer's disease. *Alzheimers Dement (Amst)* 2015;1:420–28 [CrossRef Medline](#)
  31. Wahlin A, Ambarki K, Birgander R, et al. Intracranial pulsatility is associated with regional brain volume in elderly individuals. *Neurobiol Aging* 2014;35:365–72 [CrossRef Medline](#)
  32. Birnefeld J, Wahlin A, Eklund A, et al. Cerebral arterial pulsatility is associated with features of small vessel disease in patients with acute stroke and TIA: a 4D flow MRI study. *J Neurol* 2020;267:721–30 [CrossRef Medline](#)
  33. Kockelkoren R, Vos A, Hecke WV, et al. Computed tomographic distinction of intimal and medial calcification in the intracranial internal carotid artery. *PLoS One* 2017;12:e0168360–11 [CrossRef](#)
  34. Van Den Beukel TC, Van Der Toorn JE, Vernooij MW, et al. Morphological subtypes of intracranial internal carotid artery arteriosclerosis and the risk of stroke. *Stroke* 2022;53:1339–47 [CrossRef Medline](#)
  35. Melgarejo JD, Vernooij MW, Ikram MA, et al. Intracranial carotid arteriosclerosis mediates the association between blood pressure and cerebral small vessel disease. *Hypertension* 2023;80:618–28 [CrossRef Medline](#)
  36. Tsao CW, Pencina KM, Massaro JM, et al. Cross-sectional relations of arterial stiffness, pressure pulsatility, wave reflection, and arterial calcification. *Arterioscler Thromb Vasc Biol* 2014;34:2495–500 [CrossRef Medline](#)
  37. Jansen RS, Duijst S, Mahakena S, et al. ABCC6-mediated ATP secretion by the liver is the main source of the mineralization inhibitor inorganic pyrophosphate in the systemic circulation: brief report. *Arterioscler Thromb Vasc Biol* 2014;34:1985–89 [CrossRef Medline](#)
  38. Dedinszki D, Szeri F, Kozak E, et al. Oral administration of pyrophosphate inhibits connective tissue calcification. *EMBO Mol Med* 2017;9:1463–70 [CrossRef Medline](#)
  39. Ziegler SG, Ferreira CR, MacFarlane EG, et al. Ectopic calcification in pseudoxanthoma elasticum responds to inhibition of tissue-nonspecific alkaline phosphatase. *Sci Transl Med* 2017;9:eaa1669 [CrossRef Medline](#)
  40. Bartstra JW, de Jong PA, Kranenburg G, et al. Etidronate halts systemic arterial calcification in pseudoxanthoma elasticum. *Atherosclerosis* 2020;292:37–41 [CrossRef Medline](#)
  41. Kranenburg G, de Jong PA, Bartstra JW, et al. Etidronate for prevention of ectopic mineralization in patients with pseudoxanthoma elasticum. *J Am Coll Cardiol* 2018;71:1117–26 [CrossRef Medline](#)
  42. Vernooij MW, Ikram MA, Tanghe HL, et al. Incidental findings on brain MRI in the general population. *N Engl J Med* 2007;357:1821–28 [CrossRef Medline](#)